Supplementary Information

Large-Scale Synthesis of Iron Ore@Biomass Derived ESBC to Degrade Tetracycline Hydrochloride for Heterogeneous Persulfate Activation

Tingting Tian [1,2], Xinfeng Zhu [1,*], Zhongxian Song [1], Xindong Li [2], Jinhui Zhang [1], Yanli Mao [1], Junfeng Wu [1], Wei Zhang [3,*] and Chaohai Wang [1,4,*]

[1]   Henan Key Laboratory of Water Pollution Control and Rehabilitation Technology, School of Environmental and Municipal Engineering, Henan University of Urban Construction, Pingdingshan 467036, China
[2]   School of Civil and Surveying Engineering, Jiangxi University of Science and Technology, Ganzhou 341000, China
[3]   School of Ecology and Environmental, Zhengzhou University, Zhengzhou 450001, China
[4]   Jiangsu Key Laboratory of Chemical Pollution Control and Resources Reuse, School of Environmental and Biological Engineering, Nanjing University of Science and Technology, Nanjing 210094, China
*   Correspondence: zhuxf780@163.com (X.Z.); zhangwei88@zzu.edu.cn (W.Z.); chaohai@hncj.edu.cn (C.W.)

Supplementary captions:

Table S1. Application of iron-carbon composites in water treatment

Text S1 Detection of reactive free radicals in EPR

Figure S1 Magnetic hysteresis loop of IO and IO@ESBC.

Figure S2 The XRD pattern of IO@ESBC after reaction

Figure S3 The Raman spectra of IO@ESBC after reaction

Figure S4 The pH change record of the aqueous solution at various original pH.

Figure S5 Effect of the fulvic acid (ranging from 0 mg/L to 15 mg/L) on TCH removal efficiency.

Figure S6. TOC removal in IO@ESBC/PS/TCH system. Experimental conditions: IO@ESBC dosage of 1.25 g/ L, the original PS concentration of 10 mmol/L, TCH dosage of 50 mg/L, initial pH, and temperature of 25 ℃.

Figure S7. Reaction rate curve of IO@ESBC/PS/TCH system.

Table S1 Application of iron-carbon composites in water treatment

Catalyst	Synthesis method	Oxidants	Pollutants	Removal ratio
Fe@porous Carbon [1]	NH$_2$-MIL-53(Fe) drived	PS 0.65 mM	ACV 10 mg/L	95.60% in 60 min
Fe@PB5 [2]	Fe-rich Hyperaccumulator-derived biochar	PS 5 mM	IMI 10 mg/L	90.00% in 360 min
Fe@C-800 [3]	Fe (Hbidc) drived	PS 0.2 mM	SMX 10 mg/L	98.40% in 90 min
Iron/carbon [4]	MIL-88A drived	PS 5 mM	RB 30 mg/L	Successfully decolorized of RB
Fe@Ti/C [5]	Ilmenite was carbothermal reduction via microwave irradiation	PS 10 mM	Rhodamine B 200 mg/L	94.01% in 30 min
Fe$_x$Co$_y$@C [6]	Fe$_y$Co$_{1-y}$[Co(CN)$_6$]$_{0.67}$•nH$_2$O nanospheres drived	PMS 0.2 g/L	Bisphenol A	98.00% in 30 min
FeS@BC [7]	FeS and sawdust biochar combined	PS 10 mM	TC 200mg/L	87.40% in 30 min
Fe-Mn@BC [8]	Fe-Mn and cypress sawdust combined	PS 2 g/L	AR88 250 mg/L	98.84% in 120 min
FM-SDBC [9]	Fe-Mn and sludge	PS	Orange G	75.23% in

Catalyst	Synthesis method	Oxidants	Pollutants	Removal ratio
	biochar combined	6 mM	1500 mg/L	25 h
Fe$_3$O$_4$@C/CNFs	Fe$_3$O$_4$ grafted on	PS	Ibuprofen	100% in
[10]	carbon nanofibers	1 mM	25 μM	120 min
nZVI-Ni@BC	nZVI-Ni and maize	PS	Trichloroethylene	98.90% in
[11]	straws biochar combined	4 mM	0.15 mM	60 min
Fe/g-C$_3$N$_4$ [12]	Ferrocene-modified	PS	Tetracycline	90.50% in
	graphite phase	2.5 mM	40 mg/L	60 min
	carbon nitride			

Text S1 Detection of reactive free radicals in EPR

The reactive free radicals (SO$_4^{\bullet-}$, •OH, O$_2^-$ and ^{1}O$_2$) were detected by the EPR spectrometer. 100 mM DMPO was added into a 150 mL tapered conical flask, which contained 10 mM of PS, 50 mg/L of TCH and 1.25 g/L of IO@ESBC sample. Then, the conical flasks containing mixing slurry were placed on a thermostatic shaker with a rotary speed of 240 rpm at a constant temperature of 25°C. After 10 minutes of reaction ,0.5mL of the reaction suspension were quickly withdrawn from the slurry, then filtered by membrane (0.22 μm) to obtain the filtrate. The filtrate was used to detect the signal of SO$_4^{\bullet-}$, •OH and O$_2^{\bullet-}$. The procedure of capturing the signal of ^{1}O$_2$ by 50μM TEMP was the same as before, but the difference was that additional methanol needs to be added into the filtrate in order to eliminate the interference of other free radical signals.
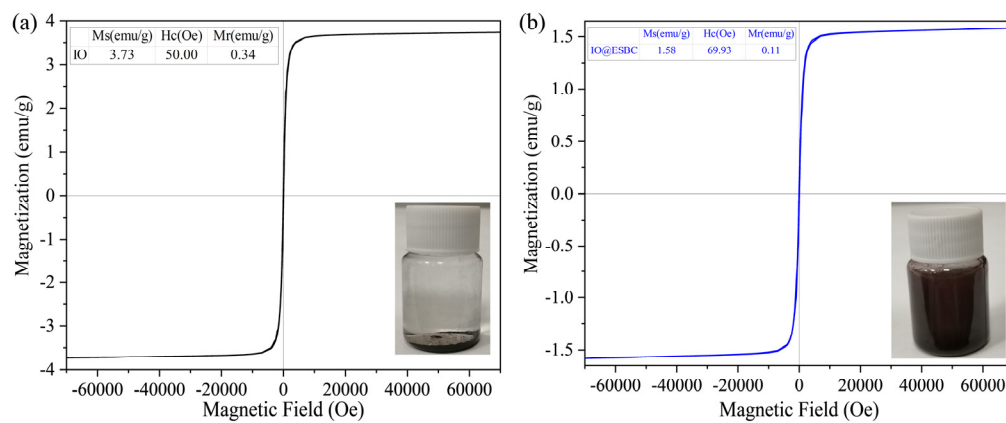
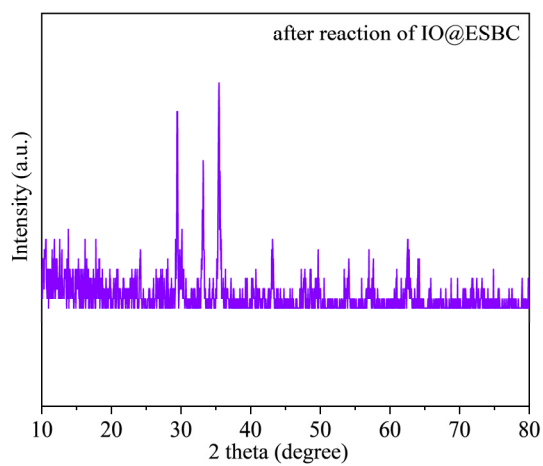**Figure S1.** Magnetic hysteresis loop of (a) IO and (b) IO@ESBC.

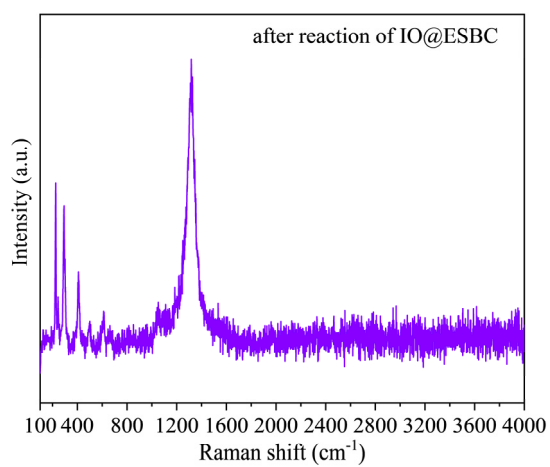**Figure S2.** The XRD pattern of IO@ESBC after reaction

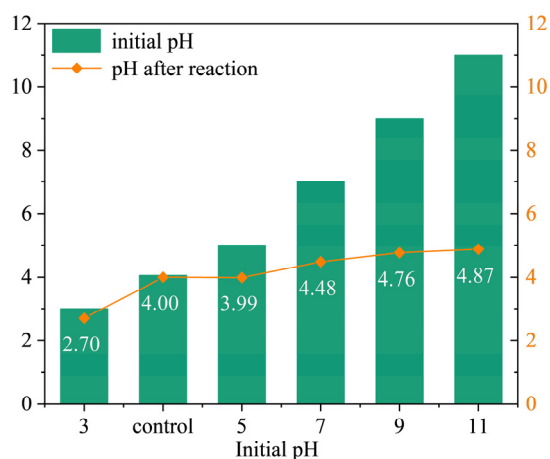**Figure S3.** The Raman spectra of IO@ESBC after reaction

Figure S4. The pH change record of the aqueous solution at various original pH. Experimental conditions: the original PS concentration of 10 mM, TCH dosage of 50 mg/L, IO@ESBC dosage of 1.25 g/L, and temperature of 25 ℃.
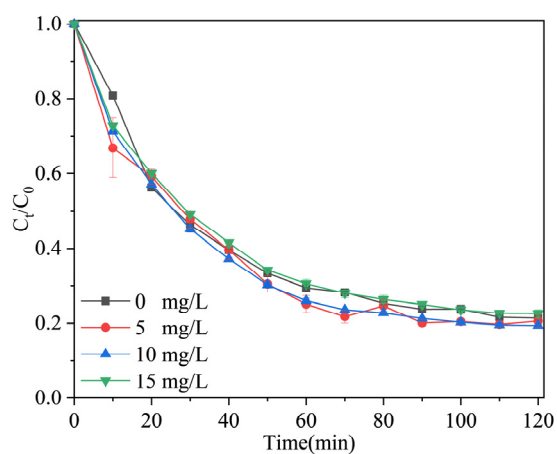

Figure S5 Effect of the fulvic acid (ranging from 0 mg/L to 15 mg/L) on TCH removal efficiency. Experimental conditions: IO@ESBC dosage of 1.25 g/ L, the original PS concentration of 10 mmol/L, TCH dosage of 50 mg/L, initial pH, and temperature of 25 ℃.

Figure S6. TOC removal in IO@ESBC/PS/TCH system. Experimental conditions:

IO@ESBC dosage of 1.25 g/ L, the original PS concentration of 10 mmol/L, TCH dosage of 50

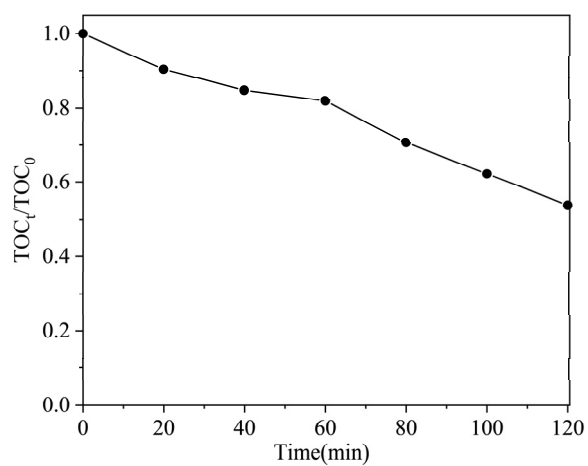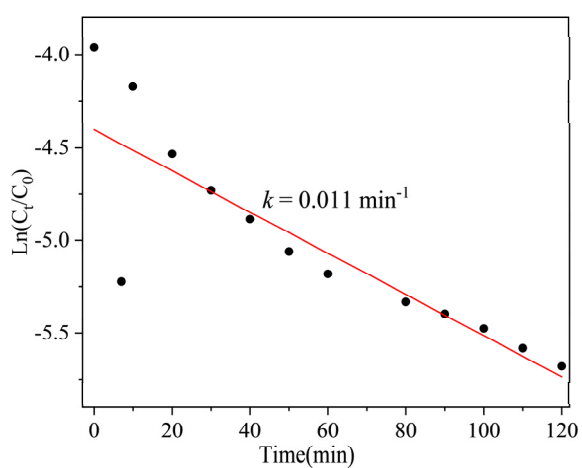mg/L, initial pH, and temperature of 25 ℃.

Figure S7. Reaction rate curve of IO@ESBC/PS/TCH system.

References

1. Liu, C.; Wang, Y.; Zhang, Y.; Li, R.; Meng, W.; Song, Z.; Qi, F.; Xu, B.; Chu, W.; Yuan, D.; Yu, B., Enhancement of Fe@porous carbon to be an efficient mediator for peroxymonosulfate activation for oxidation of organic contaminants: Incorporation NH2-group into structure of its MOF precursor. *Chemical Engineering Journal* 2018, *354*, 835-848.

2. Wang, X.; Zhang, P.; Wang, C.; Jia, H.; Shang, X.; Tang, J.; Sun, H., Metal-rich hyperaccumulator-derived biochar as an efficient persulfate activator: Role of intrinsic metals (Fe, Mn and Zn) in regulating characteristics, performance and reaction mechanisms. *Journal of Hazardous Materials* 2022, *424*, 127225.

3. Pu, M.; Wan, J.; Zhang, F.; Brusseau, M. L.; Ye, D.; Niu, J., Insight into degradation mechanism of sulfamethoxazole by metal-organic framework derived novel magnetic Fe@C composite activated persulfate. *Journal of Hazardous Materials* 2021, *414*, 125598.

4. Andrew Lin, K.-Y.; Hsu, F.-K., Magnetic iron/carbon nanorods derived from a metal organic framework as an efficient heterogeneous catalyst for the chemical oxidation process in water. *RSC Advances* 2015, *5, (63)*, 50790-50800.

5. Xie, R.; Jiang, Y.; Armutlulu, A.; Shen, Z.; Lai, B.; Wang, H., One-step fabrication of oxygen vacancy-enriched Fe@Ti/C composite for highly efficient degradation of organic pollutants through persulfate activation. *Journal of Colloid and Interface Science* 2021, *583*, 394-403.

6. Li, X.; Rykov, A. I.; Zhang, B.; Zhang, Y.; Wang, J., Graphene encapsulated FexCoy nanocages derived from metal–organic frameworks as efficient activators for peroxymonosulfate. *Catalysis Science & Technology* 2016, *6, (20)*, 7486-7494.

7. He, J.; Tang, J.; Zhang, Z.; Wang, L.; Liu, Q.; Liu, X., Magnetic ball-milled FeS@biochar as persulfate activator for degradation of tetracycline. *Chemical Engineering Journal* 2021, *404*, 126997.

8. Chen, L.; Jiang, X.; Xie, R.; Zhang, Y.; Jin, Y.; Jiang, W., A novel porous biochar-supported Fe-Mn composite as a persulfate activator for the removal of acid red 88. *Separation and Purification Technology* 2020, *250*, 117232.

9. Hao, H.; Zhang, Q.; Qiu, Y.; Meng, L.; Wei, X.; Sang, W.; Tao, J., Insight into the degradation of Orange G by persulfate activated with biochar modified by iron and manganese oxides: Synergism between Fe and Mn. *Journal of Water Process Engineering* 2020, *37*, 101470.

10. Zhang, Y.; Zhang, B.-T.; Teng, Y.; Zhao, J.; Sun, X., Heterogeneous activation of persulfate by carbon nanofiber supported Fe3O4@carbon composites for efficient ibuprofen degradation. *Journal of Hazardous Materials* 2021, *401*, 123428.

11. Shan, A.; Idrees, A.; Zaman, W. Q.; Abbas, Z.; Ali, M.; Rehman, M. S. U.; Hussain, S.; Danish, M.; Gu, X.; Lyu, S., Synthesis of nZVI-Ni@BC composite as a stable catalyst to activate persulfate: Trichloroethylene degradation and insight mechanism. *Journal of Environmental Chemical Engineering* 2021, *9, (1)*, 104808.

12. Wang, Z.; Wang, H.; Wang, Z.; Huang, D.; Qin, H.; He, Y.; Chen, M.; Zeng, G.; Xu, P., Ferrocene modified g-C3N4 as a heterogeneous catalyst for photo-assisted activation of persulfate for the degradation of tetracycline. *Colloids and Surfaces A: Physicochemical and Engineering Aspects* 2021, *626*, 127024.